Step length and the extrapolated center of mass co-vary to stabilize the margin of stability in the anterior-posterior direction during unobstructed and obstructed walking

Ashwini Kulkarni, Chuyi Cui, Shirley Rietdyk, Satyajit Ambike

Department of Health and Kinesiology, Purdue University, West Lafayette, IN

Keywords: proactive adaptation; adaptive gait; uncontrolled manifold; obstacle crossing

Address for correspondence:

Satyajit Ambike

Department of Health and Kinesiology,

800 West Stadium Ave,

Purdue University,

West Lafayette, IN 47907

USA

Tel: (765) 496-0567

E-mail: sambike@purdue.edu

ABSTRACT

During steady-state gait, the instantaneous passive dynamics, quantified using the margin of stability in the anterior-posterior (AP) direction (MOS_{AP}), are unstable. Although the instability indicates that substantial control will be required to reject a perturbation, the instability also allows for forward progression with low energy expenditure when the gait is unperturbed. Here, we examined whether humans control MOS_{AP} to exploit the passive dynamics, and whether they adjust MOS_{AP} when the threat to AP balance is increased. We computed MOS_{AP} for six consecutive steps when healthy young adults performed unobstructed gait trials, and when they approached and crossed an obstacle. Uncontrolled manifold analysis indicated that the extrapolated center of mass and step length co-varied to maintain MOS_{AP} for all steps during unobstructed and obstructed gait. Furthermore, the MOS_{AP} values indicated unstable passive dynamics for all steps except while crossing the obstacle with the leading limb. Based on these results, we concluded that the MOS_{AP} is controlled to exploit the passive dynamics and achieve forward progression at low energetic cost. Finally, MOS_{AP} increased (indicating more stable dynamics) while approaching and crossing the obstacle with the leading limb, and then declined for later steps, indicating a fluid tradeoff between stability and energy efficiency.

1. Introduction

The margin of stability (MOS), based on the inverted-pendulum model of gait, measures the instantaneous passive dynamic stability of gait [1]. During stable, unobstructed walking, MOS values in the anterior-posterior (AP) direction (MOS_{AP}) indicate unstable passive dynamics over the gait cycle [2, 3], which has led some to question the utility of MOS_{AP} as a measure of gait stability [4]. However, MOS_{AP} also reflects walking energetics. Instantaneous AP instability, particularly at heel contact [5-7], indicates that the body has sufficient momentum to passively rotate about and over the ankle of the just-placed foot, and achieve forward progression at low energetic cost [8]. Here, we propose that humans select step length to exploit these passive dynamics. Further, we propose the novel hypothesis that the central nervous system actively controls MOS_{AP} at each heel contact.

Adopting a passively unstable gait will promote forward progression on a clear, level walkway, but alterations in this strategy may arise when humans proactively adapt to navigate environmental features. When a locomotor task involves a higher risk of a forward loss of balance, reducing the dynamic instability in the anterior direction may be expedient [7]. Anterior instability during obstacle crossing is indeed lower compared to unobstructed gait [9], suggesting that stability is prioritized over energy optimality. Furthermore, it is feasible that preparatory changes in gait stability occur in the steps leading up to the obstacle (i.e., approach steps) to facilitate the transition from unobstructed to obstructed gait. In the approach steps, visual information about the hazard is being gathered [10, 11] and spatio-temporal gait characteristics (gait speed and foot placement variability) are modified [12]. However, proactive stability adaptations during approach have not been examined, and it is likely that these

stability adaptations are a critical component of maintaining forward progression through challenging environments.

Therefore, our first goal was to establish that MOS_{AP} is controlled during unobstructed as well as obstructed walking. Our second goal was to quantify any proactive adaptations in MOS_{AP} during the approach steps. We computed the MOS_{AP} at multiple consecutive heel contacts during unobstructed walking and during an obstacle-crossing task. MOS_{AP} value at heel contact is the distance from the anterior boundary of the base of support (the leading heel) to the extrapolated center of mass, or XcoM, which reflects the center of mass (CoM) state [13]. To address our first goal, we employed the uncontrolled manifold (UCM) method [14]. For each heel contact, we parsed the across-trial variance in the step length and the XcoM into two components: one that maintained MOS_{AP} (called V_{UCM}) and another that changed MOS_{AP} (called V_{ORT}). We used the normalized excess of V_{UCM} over V_{ORT} as a synergy index. A positive synergy index indicates that MOS_{AP} was actively controlled, i.e., stabilized at the specific across-trail mean MOS_{AP} for that step. A higher value indicates a stronger synergy or higher stability of MOS_{AP}. We emphasize that stability of MOS_{AP} is different from the stability of gait. MOS_{AP} is a measure of gait stability. In contrast, the synergy index indicates how effective the control was at stabilizing or maintaining MOS_{AP} at a specific value for a given step. In other words, the synergy index indicates how well the central nervous system responds to changes in XCoM with a corresponding correction in step length so that the MOS_{AP} itself is invariant. To address our second goal, we compared the MOS_{AP} values for the steps leading up to, while crossing and then resuming unobstructed gait after crossing an obstacle.

We hypothesized that the synergy index will be greater than zero (H1), indicating that the step length and the XcoM co-vary to stabilize MOS_{AP} for all steps in both tasks. We also hypothesized a task by step interaction for the synergy index (H2). The synergy index will not be different across tasks (unobstructed and obstructed) for the steps at the start and end of the walkway, but the synergy index will be lower while crossing an obstacle placed in the middle of the walkway. The lower synergy index will reflect the greater difficulty associated with the crossing steps; larger muscle activations required for stepping over the obstacle [15] will be associated with greater noise [16], which will make stabilization more difficult. We also hypothesized a task by step interaction for MOS_{AP} (H3). The MOS_{AP} will not be different across tasks for the steps at the start and end of the walkway, but the MOS_{AP} will be higher for the approach steps 1-2 steps before the obstacle and for the crossing steps. These changes are consistent with prioritization of safety over energy optimality [17]. Finally, we identified the changes in spatiotemporal gait measures that resulted in any putative changes in MOS_{AP}.

2. Methods

2.1 Participants

Twenty-six healthy young adults participated in the study. We excluded six participants due to poor kinematic tracking. Data from 20 participants (14 females, 22.3 ± 3.7 years, 1.7 ± 0.1 m, 66.9 ± 14.6 kg) were used for analysis. All participants walked without aid, had no orthopedic, neuromuscular, or dementia disorders, and were independent in daily activities. Vision was normal or corrected-to-normal. The study was approved by the University's Institutional Review Board, and all participants provided written informed consent.

2.2 Equipment and Procedures

Participants walked at their self-selected speed on a 6 m walkway and stepped over an obstacle when present (figure 1A). The obstacle was 100 cm wide × 0.8 cm deep. The height of the obstacle was scaled to 25% of the participant's leg length. The obstacle was made of black Masonite and designed to tip if contacted. The starting position was determined for each subject such that they took five steps before reaching the obstacle, crossed the obstacle with the right leg first and stopped three to four steps later (figure 1A).

Participants performed 20 trials each of walking with an obstacle (obstacle-crossing task) and walking without an obstacle (no obstacle task). We collected kinematic data at 100 Hz with a motion capture system (Vicon Vero, Oxford, UK) with marker clusters placed bilaterally on the lower back, thigh, shank, and foot. We digitized the joint centers to identify their locations relative to the marker clusters. We also digitized the top edge of the obstacle to identify its position.

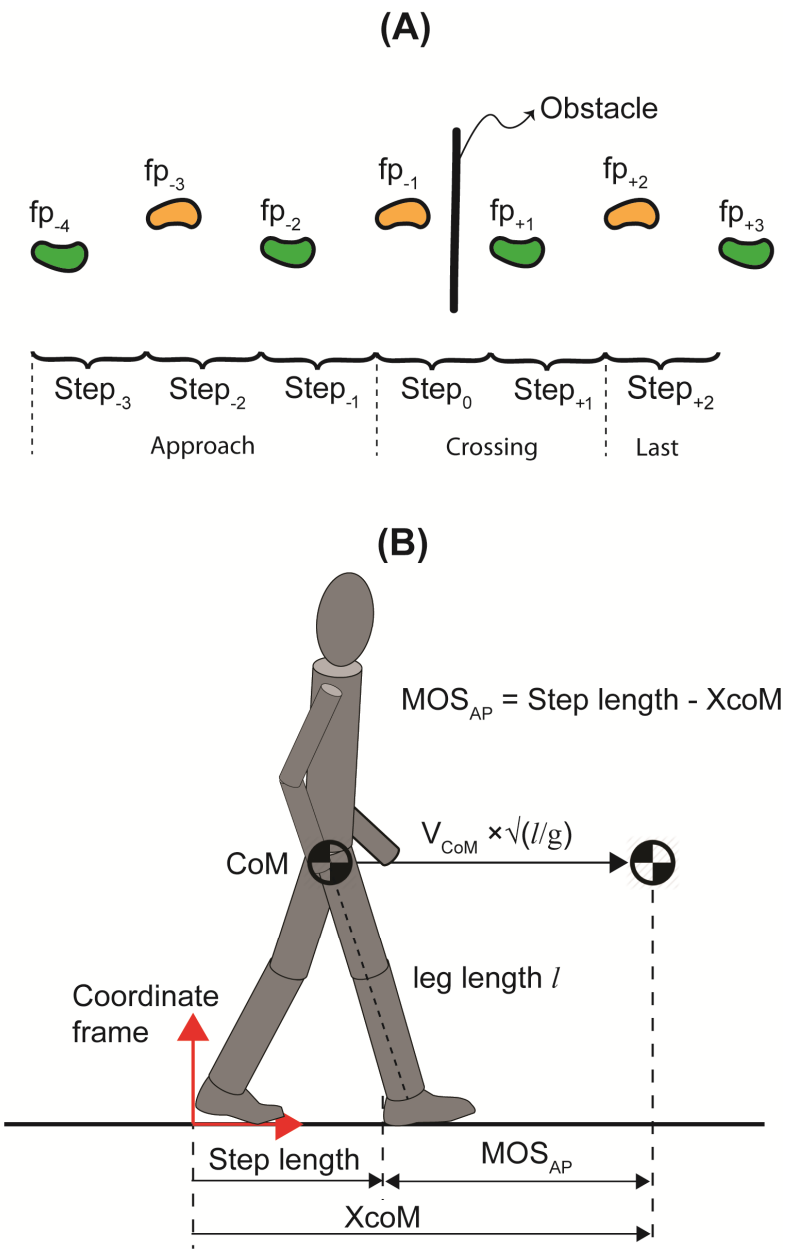

Figure 1. (A) Illustration of foot placements while approaching (fp_{-4} to fp_{-1}), crossing (fp_{+1} and fp_{+2}) and after crossing (fp_{+3}) the obstacle, and of steps while approaching ($Step_{-3}$ to $Step_{-1}$), crossing ($Step_0$ and $Step_{+1}$) and after crossing ($Step_{+2}$) the obstacle. **(B)** Definitions of the extrapolated center of mass (XcoM) and margin of stability, MOS_{AP}. Step length, XcoM and MOS_{AP} are computed at the moment of lead heel contact in a coordinate frame located where the rear heel contacted the ground.

2.3 Analysis

Some trials were discarded due to poor kinematic tracking. To have the same number of trials for all participants and tasks, we selected 15 trials with good kinematic data. Fifteen trials is sufficient for reliable quantification of the synergy variables [18]. We filtered all kinematic data using a zero-lag, 4th order, low-pass Butterworth filter with a cut-off of 7 Hz. We identified seven foot placements (figure 1A) using the AP position data of the heel markers [19]. We quantified spatiotemporal gait parameters and margin of stability at heel contact at the seven foot placements (fp_{-4} to fp_{+3}) and six steps ($Step_{-3}$ to $Step_{+2}$; figure 1A). Step length was defined as the distance between two consecutive heel contacts. CoM position was computed as the center of the geometric triangle formed by two ASIS and the center of PSIS [20]. CoM velocity was calculated by differentiating the CoM position data. The extrapolated center of mass (XcoM) was calculated in the sagittal plane as [13]:

$$XcoM = CoM + \frac{V_{CoM}}{\sqrt{\frac{g}{l}}},$$

where CoM is the anterior-posterior position of the CoM, V_{CoM} is the anterior-posterior velocity of the CoM, g is the acceleration due to gravity, and l is the participant's leg length (figure 1B). Leg length was calculated as the sagittal-plane distance between the CoM and the ankle of the limb that made contact with the ground. We used the average of the leg length values obtained from the 15 trials for each step [21]. We computed MOS_{AP} at the instant of leading heel contact in a coordinate frame fixed at the location of the rear heel contact (figure 1B):

$$MOS_{AP} = Step\ length - XcoM, \qquad (Eq. 1)$$

i.e., the distance from the anterior boundary of the base of support (BOS), defined by the position of the leading heel, to the XcoM. Positive MOS_{AP} indicates instantaneous passive stability (XcoM is behind the anterior boundary of the BOS), and negative MOS_{AP} indicates instantaneous passive instability (XcoM ahead of the anterior boundary of the BOS) in the gait.

We used the uncontrolled manifold analysis to quantify the synergy stabilizing MOS_{AP} at heel contact. We evaluate the hypothesis that the input variables (i.e., step length and XcoM), co-vary to stabilize the output variable (i.e., MOS_{AP}). We first obtain from the constraint equation (Eq. 1), the Jacobian matrix that relates small changes in the step length and XcoM to small changes in MOS_{AP}: J = [1 -1]. The one-dimensional null space of this Jacobian defines the UCM, and its one-dimensional compliment defines the orthogonal (ORT) manifold. The deviation in the step length and XcoM for each trial from the across-trial mean was projected onto the UCM and the ORT manifolds. The variances in these projections are the V_{UCM} and the V_{ORT}, respectively. These variance components are used to obtain the synergy index:

$$\Delta V = \frac{V_{UCM} - V_{ORT}}{\left(\frac{V_{UCM} + V_{ORT}}{2}\right)}.$$

The synergy index ΔV ranges from -2 to 2. Therefore, it was z-transformed for statistical analysis:

$$\Delta Vz = \frac{1}{2} * \log\left[\frac{2 + \Delta V}{2 - \Delta V}\right].$$

Note that $\Delta V = 0$ translates to $\Delta Vz = 0$. Therefore, $\Delta Vz > 0$ indicates the presence of covariation in the step length and XcoM that stabilizes MOS_{AP}. Conversely, $\Delta Vz < 0$ indicates the presence

of an anti-synergy [22] that works to change MOS_{AP}. $\Delta Vz = 0$ indicates that there is no task-specific covariation in the step length and XcoM.

2.4 Statistical analysis

To determine if the synergies were present, we performed separate, one-sample t-tests to determine if ΔVz was significantly different from zero for each step in the two tasks (H1). To determine if the gait task and foot placement affected the synergy index and MOS_{AP}, we performed a two-way (task × step) repeated measures ANOVA on the MOS_{AP} synergy index (H2) and MOS_{AP} (H3), respectively. To identify the source of changes in the synergy index and in MOS_{AP}, we performed the same ANOVA separately on the variance components (V_{UCM}, V_{ORT}), and on the CoM position, CoM velocity at heel contact and step length, respectively. For all ANOVA tests, we fit a generalized linear model with nested random effects. For the ANOVA on UCM variables and step length, the participant was the random effect. For all other variables, the trial number within each participant was the random effect. Tukey-Kramer adjustments were used to perform planned pairwise comparisons. Pairwise comparisons were conducted as follows: (1) across the two tasks for each of the six steps (or seven foot placements) and (2) across steps (or foot placements) for the obstacle-crossing task only. All analyses were performed using the PROC GLIMMIX procedure in SAS 9.4 (Cary, NC, USA) with significance set at 0.05.

3. Results

Figure 2 shows data from one participant, and illustrates changes in various outcome variables while approaching, crossing and resuming gait after crossing an obstacle, and how the variables compare with unobstructed gait for each step. These data represent the overall results. The synergy index was greater than zero (supporting H1), indicating that the step length and the XcoM co-varied to stabilize MOS_{AP} for all steps in both tasks. All outcome variables showed a task × step interaction (supporting H2 and H3) indicating that the pattern of changes in the variables across steps was different for the obstacle-crossing task compared to the no obstacle task. The largest across-task changes were observed in all outcomes for the two crossing steps ($Step_0$ and $Step_{+1}$), and some across-task changes were apparent in the approach to the obstacle ($Step_{-3}$ to $Step_{-1}$). All variables showed across-step changes for the obstacle-crossing task. In the detailed results below, we first present the results for the UCM outcome variables describing the stability of MOS_{AP}. We then present the results for MOS_{AP}, followed by results for the variables that constitute MOS_{AP}: CoM position relative to front heel, CoM velocity at heel contact, and step length.

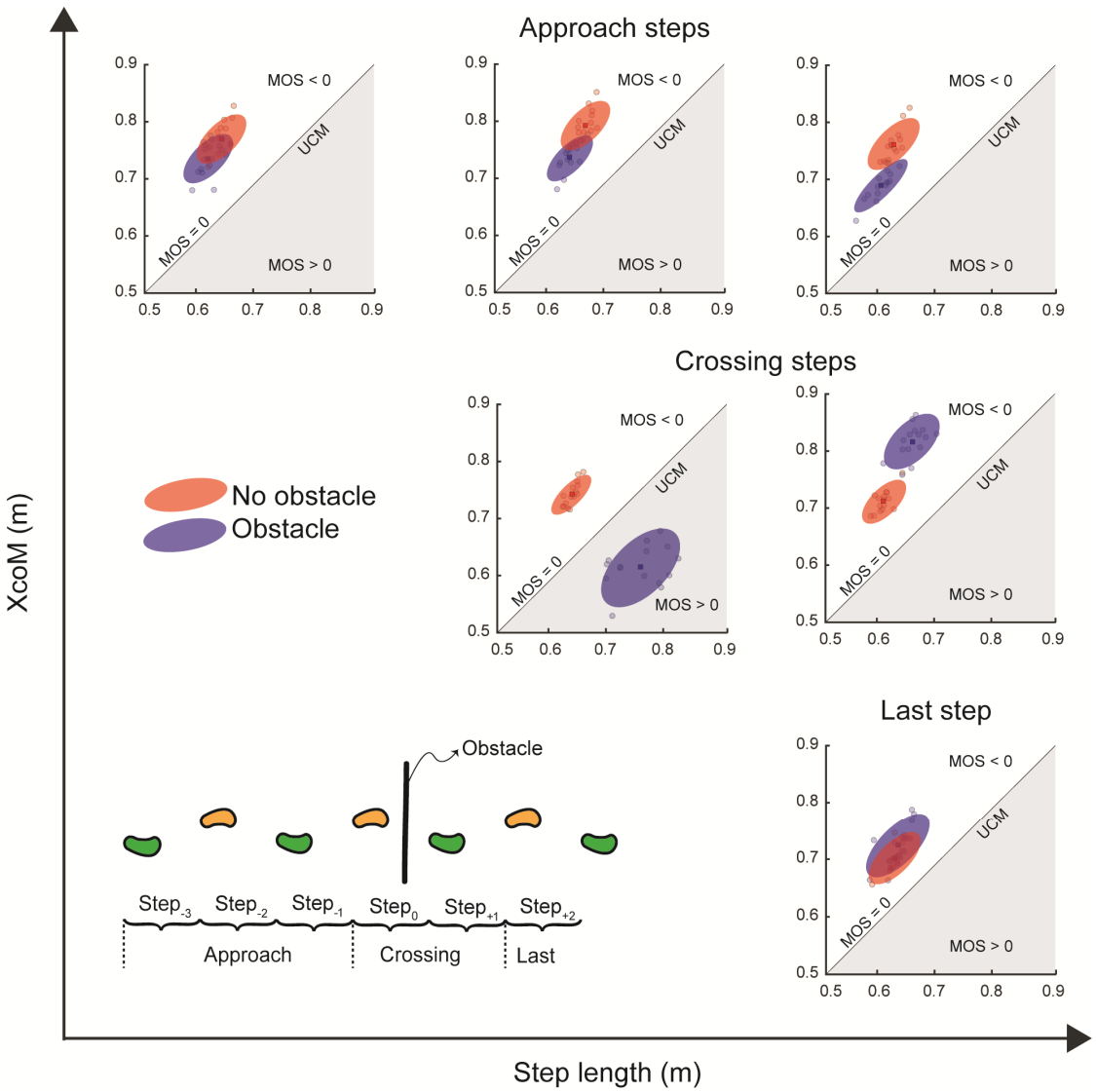

Figure 2. Data from one representative participant illustrates changes in various outcomes while approaching and crossing an obstacle, and then resuming unobstructed gait. Steps during unobstructed gait are included for comparison. The 45° line separates the regions of positive and negative MOS_{AP}; the white region above the line represents passively unstable behavior, and the gray region below the line represents passively stable behavior. The 45° line also represents the uncontrolled manifold (UCM). Variations in step length and XcoM along this direction do not change MOS_{AP}. The ellipses are centered at the centroid of the across-trial data for each step, and the major axes are aligned with the 45° line. However, the flatness of the ellipses is representative. Location of the ellipses indicates the mean MOS_{AP}. The flatness of the ellipse reflects the synergy index, with flatter ellipses indicating higher synergy indices that reflect stronger covariation between the step length and XcoM.

3.1 UCM variables

Synergy index

The synergy index (ΔVz) was significantly greater than zero at all steps for both tasks ($t_{19} < 15.97$, $p < 0.01$; figure 3A).

We observed a task × step interaction for the synergy index ΔVz ($F_{5,209} = 2.89$, $p = 0.015$; $\eta_p^2 = 0.3$; figure 3A). Post-hoc comparisons across tasks revealed that ΔVz was lower during the obstacle-crossing task compared to the no obstacle task for the lead ($step_0$) and trail crossing steps ($step_{+1}$). Post-hoc comparisons across steps for the obstacle-crossing task revealed that ΔVz was lower at the lead crossing step ($step_0$) compared to all non-crossing steps except $step_{-2}$, and ΔVz was lower at the trail crossing step ($step_{+1}$) compared to the last step ($step_{+2}$).

Variance components

We observed a task × step interaction for V_{UCM} ($F_{5,209} = 3.12$, $p = 0.009$; $\eta_p^2 = 0.3$; figure 3B). Post-hoc comparisons across tasks revealed that V_{UCM} was higher for the obstacle-crossing task compared to the no obstacle task at all but the first two steps ($step_{-3}$ and $step_{-2}$). Post-hoc comparisons across steps for the obstacle-crossing task revealed that V_{UCM} was higher at the lead crossing step ($step_0$) compared to the first two steps ($step_{-3}$ and $step_{-2}$).

We observed a task × step interaction for V_{ORT} ($F_{5,209} = 16.51$, $p < 0.001$; $\eta_p^2 = 0.3$; figure 3C). Post-hoc comparisons across task revealed that V_{ORT} was higher during the obstacle-crossing task compared to the no obstacle task at the lead ($step_0$) and trail ($step_{+1}$) crossing steps. Post-hoc comparisons across steps for the obstacle-crossing task revealed that V_{ORT} was

higher at the lead crossing step ($step_0$) compared to all other steps, and V_{ORT} was higher at the trail crossing step ($step_{+1}$) compared to all steps except the lead crossing step ($step_0$) and the preceding step ($step_{-1}$).

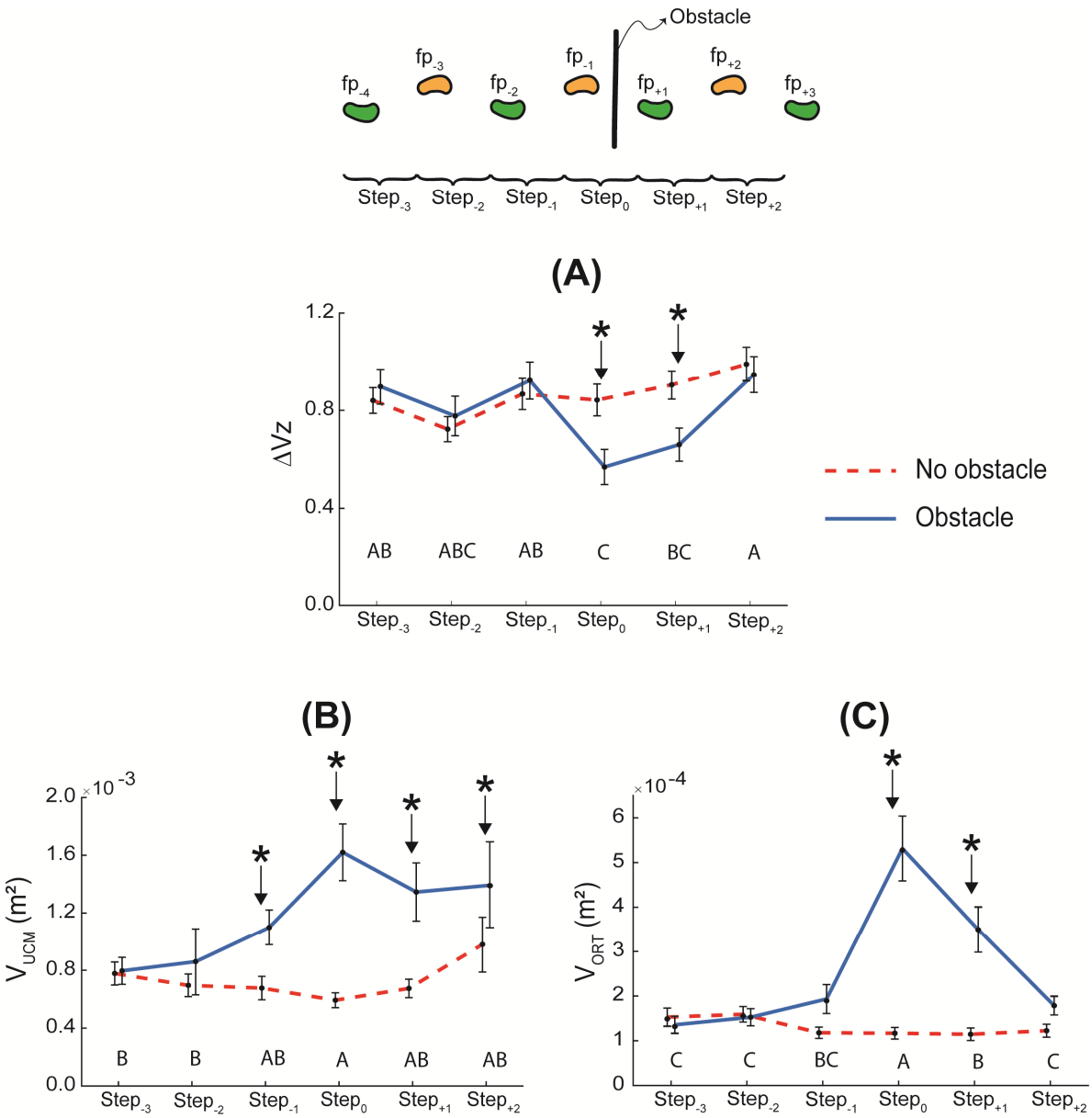

Figure 3. Mean and standard error of the MOS_{AP} synergy index **(A)**, V_{UCM} **(B)**, and V_{ORT} **(C)**. Asterisks denote significant across-task differences at that step ($p < 0.05$). Across-step pairwise comparisons for the obstacle-crossing task are indicated by the row of letters above the horizontal axis for each panel. Steps that do not have letters in common are significantly different from each other (i.e., A is different from B, but A is not different from AB).

3.2 Margin of stability

<u>MOS_{AP}</u>

We observed a task × step interaction for MOS_{AP} ($F_{6,4167} = 886.89$, $p < 0.001$; $\eta_p^2 = 0.9$; figure 4A). Post-hoc comparisons across tasks revealed that MOS_{AP} was higher (lower instability) for the obstacle-crossing task than the no obstacle task at all except the first (fp_{-4}) and last two foot placements (fp_{+2} and fp_{+3}). MOS_{AP} was more negative (greater instability) for fp_{+2} (after trail foot crossing) for the obstacle task. All pair-wise across-step comparisons for the obstacle-crossing task are depicted in figure 4A. For brevity, we describe only some of the significant differences. Changes in MOS_{AP} occurred before the obstacle was reached; MOS_{AP} was higher (lower instability) for fp_{-1} relative to the two preceding foot placements. For the two crossing steps, MOS_{AP} first changed from negative to positive for fp_{+1}, and then changed to the most negative value for fp_{+2} relative to all foot placements.

<u>CoM position relative to the rear heel</u>

A task × step interaction was observed for the CoM position relative to the rear heel ($F_{6,4167} = 391.20$, $p < 0.001$; $\eta_p^2 = 0.9$; figure 4B). Post-hoc comparisons across tasks revealed that CoM was closer to the rear heel at the foot placements of all approach steps and the lead crossing step (fp_{-4} to fp_{+1}). Conversely, CoM was closer to the front heel at the foot placement for the trail crossing step (fp_{+2}). All pair-wise across-step comparisons for the obstacle-crossing task are depicted in figure 4B. For brevity, we describe only some of the significant differences. CoM position changed for the last three foot placements. The CoM was closer to the rear foot

at the foot placement for the lead crossing step (fp_{+1}). It shifted forward, so that it was closer to the front heel at the foot placement for the trail crossing step (fp_{+2}), and then returned to a location consistent with that for the approach steps at the foot placement for the last step (fp_{+3}).

CoM velocity at heel contact

We observed a task × step interaction for the CoM velocity at heel contact ($F_{6,4167}$= 161.52, $p < 0.001$; $\eta_p^2 = 0.8$; figure 4C). Post-hoc comparisons across tasks revealed that the CoM velocity was lower for the obstacle-crossing task compared to the no-obstacle task at all but the first and the last foot placements (fp_{-4} and fp_{+3}). Post-hoc comparisons across steps for the obstacle-crossing task revealed that the CoM velocity was lower at the first (fp_{-4}) and last (fp_{+3}) foot placement compared to other foot placements, except at the lead foot crossing (fp_{+1}), where the CoM velocity was lower compared to all other foot placements.

Step length

We observed a task × step interaction for the step length ($F_{5,3569} = 149.09$; $p < 0.001$; $\eta_p^2 = 0.9$; figure 4D). Post-hoc comparisons across tasks revealed that step length was longer during the obstacle-crossing task compared to the no obstacle task at the lead ($step_0$) and trail crossing ($step_{+1}$) steps. Post-hoc comparisons across steps for the obstacle-crossing task revealed that step length increased one step before the crossing step ($step_{-1}$) compared to the first step ($step_{-3}$); it increased to the highest observed value for the lead crossing step ($step_0$). Step length then shortened for the trail crossing step ($step_{+1}$), but remained longer than all steps except $step_0$, and finally, it was the shortest for the last step ($step_{+2}$) compared to all other steps.

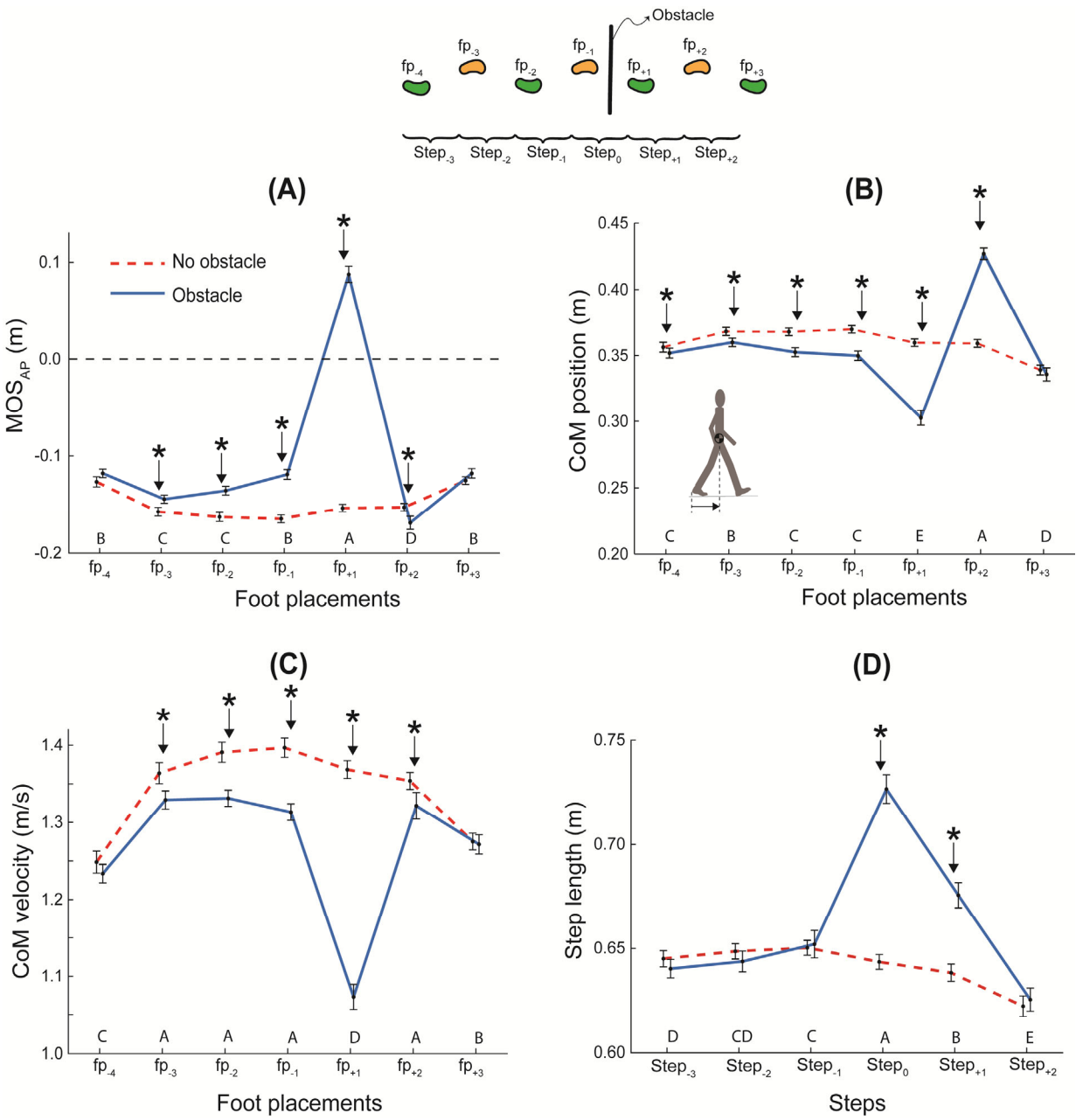

Figure 4. Mean and standard error of the MOS_{AP} **(A)**, CoM position at heel contact **(B)**, CoM velocity at heel contact **(C)** and step length **(D)**. Asterisks denote significant task difference at that step ($p < 0.05$). Across-step pairwise comparisons for the obstacle-crossing task are indicated by the row of letters above the horizontal axis for each panel. Steps that do not have letters in common are significantly different from each other (i.e., A is different from B, but A is not different from AB).

4. Discussion

Our study focused on the proactive changes to passive dynamic gait stability, quantified using MOS_{AP}, that humans implement to safely navigate a hazard. Our goals were to establish that MOS_{AP} is controlled during unobstructed as well as obstructed walking, and to quantify any proactive adaptations in MOS_{AP} during obstacle crossing. We addressed our first goal using the uncontrolled manifold analysis, which provides a synergy index that quantifies the across-trial co-variance in the step length and the XcoM – the two input variables that yield the MOS_{AP}. A positive synergy index indicates that MOS_{AP} is controlled, i.e., stabilized at a specific value. We addressed our second goal by comparing MOS_{AP} across tasks and steps. The data supported our hypotheses. The synergy index was positive for all steps in unobstructed and obstructed gait (H1), indicating that MOS_{AP} is controlled for all steps in both tasks. That is, step length was selected to account for changes in XcoM, such that the MOS_{AP} remained relatively invariant. Furthermore, the synergy index was lower while crossing an obstacle compared to earlier and later steps, and also compared to the corresponding steps during unobstructed gait (H2). We observed that MOS_{AP} changed for unobstructed versus obstructed gait, and also across steps while approaching and crossing an obstacle, and then resuming unobstructed gait (H3).

Note that hypotheses H1 and H2 focus on the synergy index and pertain to the control or stabilization of MOS_{AP} at a specific value for a given step, similar to the stabilization of a system about a set point. With hypothesis H3, we shift our attention to the actual value of MOS_{AP}, i.e., the value of that set point. MOS_{AP} quantifies the instantaneous passive stability of gait (based on an inverted-pendulum model) at heel contact, whereas the synergy index quantifies the stability of the specific value of MOS_{AP} at each step. We argue below that (1) the

positive synergy indices indicate that the passive instability is not a byproduct of another process, but that the step length is selected to exploit the unstable passive dynamics to achieve forward progression at low energetic cost; and (2) the proactive changes in the mean MOS_{AP} for the obstacle-crossing task reflect a stability-efficiency tradeoff.

4.1 The synergy analysis

<u>The synergy index provides evidence for the control of MOS_{AP}</u>

The first major finding of this study is that MOS_{AP} is a controlled variable ($\Delta Vz > 0$ for all steps; figure 3A). In particular, the synergy index remains significantly larger than zero, even though the input variables that define the MOS_{AP} change over multiple steps for the obstacle-crossing task (figures 2 and 4). Thus, the UCM analysis provides strong quantitative evidence that MOS_{AP} is controlled.

The variance components (figures 3B, C) provide information regarding the underlying processes that stabilize MOS_{AP}. Higher V_{ORT} indicates higher variability in MOS_{AP}, whereas higher V_{UCM} indicates greater compensatory covariance between XcoM and step length. We observed that MOS_{AP} is more variable for the crossing steps (up to 205% increase in V_{ORT} compared to earlier steps; figure 3C). This likely arises from the larger muscle activations and joint moments required for the crossing steps compared to unobstructed steps [15, 23]; increases in the magnitude of signal-dependent noise [16] will lead to more variable MOS_{AP}. However, this increase is offset by an increase in V_{UCM} (up to 103% increase compared to earlier steps; figure 3B). This compensation leads to MOS_{AP} stabilization overall (figure 3A).

<u>Does the synergy arise from passive mechanics, or do neural mechanisms contribute?</u>

It is unlikely that passive mechanics of the gait cycle alone can explain the presence of a synergy that stabilizes MOS_{AP}. It is indeed likely that mechanics contribute; for example, a greater push off force would result in a more anterior XcoM, but it would also tend to produce longer steps [8], thereby maintaining MOS_{AP}. However, the step length is not entirely determined by a passively swinging leg. Rather, activity in the leg muscles and powers at the hip and knee indicate active control of the forward swinging limb, which will alter the step length from what a passively swinging limb would yield [24]. It is plausible that variations in muscle lengths from their reference values, arising from variations in push off forces, will engage spinal stretch reflexes that will alter step length and contribute to the observed MOS_{AP} synergy [25]. This explanation is consistent with the view that, for steady state, level gait, humans rely on spinal feedback for control in the AP direction [26, 27].

The contribution of neural mechanisms to the MOS_{AP} synergy may be even greater for obstructed gait. We observed large fluctuations in the MOS_{AP} over the approach and crossing steps (174% increase for fp_{+1} over fp_{-1}, and a 292% decline for fp_{+2} over fp_{+1}; figure 4A). Nevertheless, the synergy index, although lower (38% decline for $Step_0$ relative $Step_{-1}$; figure 3A), remained positive. The positive synergy index despite large fluctuations in related variables over consecutive steps suggests the involvement of supraspinal mechanisms. Indeed, supraspinal centers are involved in the control of the obstacle crossing steps [15]. Spinal reflex responses in the stance leg flexors are enhanced, likely due to increased activity in the prefrontal cortex, in preparation for swinging the leg over the obstacle. Furthermore, the prefrontal cortical activity remains enhanced (compared to unobstructed walking) while swinging the leg over the obstacle [15]. It is also known that visual information about the

obstacle is gathered during approach and used to alter gait characteristics [10, 11]. Gathering and using visual information also implicates higher brain centers in the control of obstructed gait, supporting our view that the MOS_{AP} synergy arises from spinal and supraspinal neural circuits. Note that the neurophysiological bases of synergies are not known. However, both spinal and supraspinal structures are candidate mechanisms [28].

Our ideas parallel a similar proposal by Dingwell and colleagues. They investigated step-to-step changes in the MOS in the medio-lateral (ML) direction in externally destabilized environments and argued that MOS_{ML} is controlled during level walking [21, 29, 30]. The focus of previous research on ML stability – versus AP stability – is consistent with the view that level gait requires more control along the ML direction, and minimal control along the AP direction [26]. The UCM analyses performed here show that the MOS is also controlled in the AP direction through the selection of step length – not only in gait tasks that require proactive adaptations, but also during steady state gait.

4.2 Proactive changes in MOS_{AP} and the fluid compromise between stability and energy efficiency

The second major finding of this study is that the MOS_{AP} changes while approaching the obstacle. In the across-step comparisons for the obstacle-crossing task, MOS_{AP} began to increase (indicating lower instability) one step before the crossing step ($fp_{-1} > fp_{-2}$ in figure 4A). When compared to unobstructed gait, changes in MOS_{AP} for the obstacle-crossing task are apparent three steps before the obstacle. In general, speed is lower and the CoM position is more posterior during obstructed gait for several steps before reaching the obstacle (figures 4B, 4C). While these changes are apparent for the approach steps, the largest changes in MOS_{AP}

were seen for the crossing steps. For these steps, MOS_{AP} changes arose from changes in all three variables that constitute it. For example, the 174% increase in the MOS_{AP} for fp_{+1} compared to the previous heel contact (fp_{-1}) arises from 18% decline in CoM speed, a 13% shift in the CoM position towards the rear foot, and an 11% increase in step length. The MOS_{AP} alterations are consistent with previous work where changes in MOS in the anterior and medial directions were evident during the swing phase immediately prior to taking unnaturally long or quick steps [31]. It is striking that, according to our data, MOS_{AP} changes several steps before reaching the obstacle, indicating that the transition from unobstructed gait to the movements required for crossing the obstacle occurs over several steps.

The instantaneous passive dynamic instability revealed by MOS_{AP} [2, 3, 6] seems at odds with the fact that participants do not show any overt signs of unstable gait (e.g., no falls are reported in such studies). While this contradiction has led some to question the utility of MOS_{AP} for quantifying gait stability [4], changes in MOS_{AP} across steps or tasks provides relevant information about stability. In particular, passive dynamic stability is modulated in response to percieved risk [7]. For example, the substantive increase in MOS_{AP} for lead crossing (figures 2, 4A) may be a preemptive strategy against a potential trip that will lead to a forward fall [32]. Similarly, the even-more-substantive transition back – to the most unstable passive dynamics (lowest MOS_{AP}) following the trail crossing step – may be a response to the fact that the risk of a forward fall is diminished after the trail foot crosses the obstacle [33, 34]. The increased instability after trail foot crossing may reflect the exploitation of passive dynamics to propel the body forward faster, so that individuals can regain their gait speed (figure 4C).

These fluctuations in passive dynamic stability increase the eneretic cost of locomotion. The negative MOS_{AP} at heel contact indicates that the body has sufficient momentum to rotate over and about the new stance ankle without significant energy expenditure. Therefore, the increase in MOS_{AP} over approach steps, and especially the positive MOS_{AP} for the crossing step, indicates that the trailing leg must provide increaseing amounts of pushoff so that the body can rotate over and beyond the stance ankle. Furthermore, the lead crossing step ($step_0$) is a slower and longer step (figure 4C, 4D). Humans tend to vary step length in proportion to speed, so that the energetic cost of walking remains low [35]. Therefore, the opposing speed and step length changes for the crossing step, while they improve passive dynamic stability, are energetically suboptimal, likely due to increased step-to-step transition cost [36]. This means that the passive dynamic stability is improved at the cost of energy effeciency during obstacle crossing. Similar arguments have been made based on observed MOS_{AP} values during stair descent [5], as well as the the differences in the observed mechanical work during obstacle crossing and the work obtained from a model-based optimization computation for the same task [17].

In sum, inspecting changes in MOS_{AP} across tasks and steps leads to the conclusion that MOS_{AP} is proactively adjusted (1) during the approach, likely to facilitate the transition from steady-state gait to the movements required to clear the obstacle, (2) while crossing an obstacle, likely to prioritize safety over energy optimality, and (3) when resuming level gait to regain gait speed. The large fluctuations in MOS_{AP} reflect a fluid compromise between stability and energy efficiency.

4.3 Limitations

We estimated the CoM location using four pelvis markers [20]. A rigorous whole-body model could have provided slightly different estimates of the CoM motion. However, these differences would influence MOS_{AP} similarly across all conditions, and using a different method to obtain CoM kinematics would likely yield similar qualitative results and overall conclusions, especially given the large effect sizes for all our outcome variables. We also observed effects of gait initiation and termination in our data. Gait was initiated one step before the examined steps, and gait was terminated one or two steps after the trail crossing step. Using a longer walkway – with more steps before and after the obstacle – may alter the values of our outcome variables. We do not expect that these changes will influence our key conclusions (control of and proactive changes in MOS_{AP}). However, effects of gait initiation and termination on MOS_{AP} behavior may be worth an independent investigation.

5. Conclusion

We have demonstrated that the XcoM and the step length covary to maintain MOS_{AP}, indicating that MOS_{AP} is controlled during unobstructed and obstructed gait. In conjunction with the consistently negative MOS_{AP} values for most of the analyzed steps, we conclude that the MOS_{AP} is controlled to exploit the passive dynamics and achieve forward progression at low energetic cost. Furthermore, the value of MOS_{AP} is proactively altered while approaching an obstacle, and MOS_{AP} shows substantial fluctuations for the two crossing steps. These changes reflect a fluid compromise between stability and energy efficiency. The changes during approach and lead crossing steps indicate a growing preference for stability, whereas the

opposite change after the trail crossing step indicates a reversion to improving efficiency when the risk to balance is reduced. Given these new insights into AP stability, we conclude that the UCM analysis of MOS_{AP} provides relavant information regarding the control of balance during walking – especially for gait tasks requiring proactive adaptations – and the effects of age and pathology on this process.

REFERENCES

1 Hof, A. L. 2008 The 'extrapolated center of mass' concept suggests a simple control of balance in walking. *Hum Mov Sci*. **27**, 112-125. (10.1016/j.humov.2007.08.003)
2 Ohtsu, H., Yoshida, S., Minamisawa, T., Takahashi, T., Yomogida, S. I., Kanzaki, H. 2019 Investigation of balance strategy over gait cycle based on margin of stability. *J Biomech*. **95**, 109319. (10.1016/j.jbiomech.2019.109319)
3 Ohtsu, H., Yoshida, S., Minamisawa, T., Katagiri, N., Yamaguchi, T., Takahashi, T., Yomogida, S. I., Kanzaki, H. 2020 Does the balance strategy during walking in elderly persons show an association with fall risk assessment? *J Biomech*. **103**, 109657. (10.1016/j.jbiomech.2020.109657)
4 Bruijn, S. M., Meijer, O. G., Beek, P. J., van Dieen, J. H. 2013 Assessing the stability of human locomotion: a review of current measures. *J R Soc Interface*. **10**, 20120999. (10.1098/rsif.2012.0999)
5 Bosse, I., Oberlander, K. D., Savelberg, H. H., Meijer, K., Bruggemann, G. P., Karamanidis, K. 2012 Dynamic stability control in younger and older adults during stair descent. *Hum Mov Sci*. **31**, 1560-1570. (10.1016/j.humov.2012.05.003)
6 Hak, L., Hettinga, F. J., Duffy, K. R., Jackson, J., Sandercock, G. R. H., Taylor, M. J. D. 2019 The concept of margins of stability can be used to better understand a change in obstacle crossing strategy with an increase in age. *J Biomech*. **84**, 147-152. (10.1016/j.jbiomech.2018.12.037)
7 Hak, L., Houdijk, H., Beek, P. J., van Dieen, J. H. 2013 Steps to take to enhance gait stability: the effect of stride frequency, stride length, and walking speed on local dynamic stability and margins of stability. *PLoS One*. **8**, e82842. (10.1371/journal.pone.0082842)
8 Kuo, A. D., Donelan, J. M. 2010 Dynamic principles of gait and their clinical implications. *Phys Ther*. **90**, 157-174. (10.2522/ptj.20090125)
9 Raffegeau, T. E., Brinkerhoff, S. A., Kellaher, G. K., Baudendistel, S., Terza, M. J., Roper, J. A., Hass, C. J. 2022 Changes to margins of stability from walking to obstacle crossing in older adults while walking fast and with a dual-task. *Exp Gerontol*. **161**, 111710. (10.1016/j.exger.2022.111710)
10 Diaz, G. J., Parade, M. S., Barton, S. L., Fajen, B. R. 2018 The pickup of visual information about size and location during approach to an obstacle. *PLoS One*. **13**, e0192044. (10.1371/journal.pone.0192044)
11 Patla, A. E., Vickers, J. N. 1997 Where and when do we look as we approach and step over an obstacle in the travel path? *Neuroreport*. **8**, 3661-3665. (10.1097/00001756-199712010-00002)
12 Muir, B. C., Haddad, J. M., van Emmerik, R. E. A., Rietdyk, S. 2019 Changes in the control of obstacle crossing in middle age become evident as gait task difficulty increases. *Gait Posture*. **70**, 254-259. (10.1016/j.gaitpost.2019.01.035)
13 Hof, A. L., Gazendam, M. G., Sinke, W. E. 2005 The condition for dynamic stability. *J Biomech*. **38**, 1-8. (10.1016/j.jbiomech.2004.03.025)
14 Scholz, J. P., Schoner, G. 1999 The uncontrolled manifold concept: identifying control variables for a functional task. *Exp Brain Res*. **126**, 289-306.
15 Haefeli, J., Vogeli, S., Michel, J., Dietz, V. 2011 Preparation and performance of obstacle steps: interaction between brain and spinal neuronal activity. *Eur J Neurosci*. **33**, 338-348. (10.1111/j.1460-9568.2010.07494.x)

16 Harris, C. M., Wolpert, D. M. 1998 Signal-dependent noise determines motor planning. *Nature*. **394**, 780-784. (10.1038/29528)
17 Chou, L. S., Draganich, L. F., Song, S. M. 1997 Minimum energy trajectories of the swing ankle when stepping over obstacles of different heights. *J Biomech*. **30**, 115-120. (10.1016/s0021-9290(96)00111-x)
18 Rosenblatt, N. J., Hurt, C. P. 2019 Recommendation for the minimum number of steps to analyze when performing the uncontrolled manifold analysis on walking data. *Journal of biomechanics*. **85**, 218-223. (10.1016/j.jbiomech.2019.01.018)
19 Desailly, E., Daniel, Y., Sardain, P., Lacouture, P. 2009 Foot contact event detection using kinematic data in cerebral palsy children and normal adults gait. *Gait Posture*. **29**, 76-80. (10.1016/j.gaitpost.2008.06.009)
20 Whittle, M. W. 1997 Three-dimensional motion of the center of gravity of the body during walking. *Hum Movement Sci*. **16**, 347-355. (Doi 10.1016/S0167-9457(96)00052-8)
21 McAndrew Young, P. M., Wilken, J. M., Dingwell, J. B. 2012 Dynamic margins of stability during human walking in destabilizing environments. *J Biomech*. **45**, 1053-1059. (10.1016/j.jbiomech.2011.12.027)
22 Cui, C., Kulkarni, A., Rietdyk, S., Barbieri, F. A., Ambike, S. 2020 Synergies in the ground reaction forces and moments during double support in curb negotiation in young and older adults. *Journal of Biomechanics*. **106**, 109837.
23 Chou, L. S., Draganich, L. F. 1997 Stepping over an obstacle increases the motions and moments of the joints of the trailing limb in young adults. *J Biomech*. **30**, 331-337. (10.1016/s0021-9290(96)00161-3)
24 Winter, D. A. 1991 *The Bionechanics and Motor Control of Human Gait: Normal, Elderly and Pathological*. Second ed. Kitchener, ON: Waterloo Biomechanics.
25 Latash, M. L. 2021 One more time about motor (and non-motor) synergies. *Exp Brain Res*. **239**, 2951-2967. (10.1007/s00221-021-06188-4)
26 Bauby, C. E., Kuo, A. D. 2000 Active control of lateral balance in human walking. *J Biomech*. **33**, 1433-1440. (10.1016/s0021-9290(00)00101-9)
27 Collins, S. H., Kuo, A. D. 2013 Two independent contributions to step variability during over-ground human walking. *PLoS One*. **8**, e73597. (10.1371/journal.pone.0073597)
28 Tillman, M., Ambike, S. 2018 Cue-induced changes in the stability of finger force-production tasks revealed by the uncontrolled manifold analysis. *J Neurophysiol*. **119**, 21-32. (10.1152/jn.00519.2017)
29 McAndrew Young, P. M., Dingwell, J. B. 2012 Voluntarily changing step length or step width affects dynamic stability of human walking. *Gait Posture*. **35**, 472-477. (10.1016/j.gaitpost.2011.11.010)
30 Kazanski, M., Cusumano, J. P., Dingwell, J. B. 2021 Rethinking Margin of Stability: Incorporating Step-To-Step Regulation to Resolve the Paradox. *bioRxiv*.
31 Sivakumaran, S., Schinkel-Ivy, A., Masani, K., Mansfield, A. 2018 Relationship between margin of stability and deviations in spatiotemporal gait features in healthy young adults. *Hum Mov Sci*. **57**, 366-373. (10.1016/j.humov.2017.09.014)
32 Peebles, A. T., Reinholdt, A., Bruetsch, A. P., Lynch, S. G., Huisinga, J. M. 2016 Dynamic margin of stability during gait is altered in persons with multiple sclerosis. *J Biomech*. **49**, 3949-3955. (10.1016/j.jbiomech.2016.11.009)

33 Muir, B. C., Bodratti, L. A., Morris, C. E., Haddad, J. M., van Emmerik, R. E. A., Rietdyk, S. 2020 Gait characteristics during inadvertent obstacle contacts in young, middle-aged and older adults. *Gait Posture*. **77**, 100-104. (10.1016/j.gaitpost.2020.01.020)
34 Heijnen, M. J., Muir, B. C., Rietdyk, S. 2012 Factors leading to obstacle contact during adaptive locomotion. *Exp Brain Res*. **223**, 219-231. (10.1007/s00221-012-3253-y)
35 Kuo, A. D. 2001 A simple model of bipedal walking predicts the preferred speed-step length relationship. *J Biomech Eng*. **123**, 264-269. (10.1115/1.1372322)
36 Kuo, A. D., Donelan, J. M., Ruina, A. 2005 Energetic consequences of walking like an inverted pendulum: step-to-step transitions. *Exerc Sport Sci Rev*. **33**, 88-97. (10.1097/00003677-200504000-00006)

Acknowledgments

This work was supported by the Bilsland Dissertation Fellowship awarded by the Office of Interdisciplinary Graduate Programs, and Corrigan Professional Development Grant awarded by the Department of Health and Kinesiology at the university.

Additional information

Competing interests. The authors declare that they have no competing interests.